JOURNAL OF GEOPHYSICAL RESEARCH, VOL. 112, B05420, doi:10.1029/2006JB004286, 2007

Application of rate-and-state friction laws to creep compaction of unconsolidated sand under hydrostatic loading conditions

Paul Hagin,[1] Norman H. Sleep,[1] and Mark D. Zoback[1]

Received 12 January 2006; revised 6 December 2006; accepted 22 February 2007; published 30 May 2007.

[1] Rate-and-state variable friction laws describe the time-dependent fault-normal compaction that occurs during holds in slide-hold-slide friction tests on unconsolidated materials. This time-dependent deformation is qualitatively similar to that observed during volumetric creep strain tests on unconsolidated sands and shales under hydrostatic loading conditions. To test whether rate-and-state friction laws can be used to model volumetric creep processes in unconsolidated sands, the rate-and-state formulation is expanded to include deformation under hydrostatic stress boundary conditions. Results show that the hydrostatic stress form of the rate-and-state friction law successfully describes the creep strain of unconsolidated sand. More importantly, values obtained for rate-and-state friction parameters by fitting these data are in the same range as those obtained from more traditional tests by fitting the fault-normal compaction of simulated gouge during a hold in a laboratory friction experiment.

Citation: Hagin, P., N. H. Sleep, and M. D. Zoback (2007), Application of rate-and-state friction laws to creep compaction of unconsolidated sand under hydrostatic loading conditions, *J. Geophys. Res.*, *112*, B05420, doi:10.1029/2006JB004286.

1. Introduction

[2] Given that the deformation of most unconsolidated sands has been observed to depend on both state (contact area or porosity) and deformation rate, it is necessary to include these effects when constructing an appropriate constitutive law [*Yale et al.*, 1993; *Ostermeier*, 1995; *Chang et al.*, 1997; *Hagin and Zoback*, 2004]. A natural choice for such a law is the rate-and-state variable friction law, since it already contains the necessary terms and was empirically derived from laboratory observations in a concise mathematical form [e.g., *Dieterich*, 1978, 1979] and has a physical basis in thermally activated creep at high-stress asperity contacts [*Nakatani*, 2001; *Rice et al.*, 2001; *Beeler*, 2004; *Nakatani and Scholz*, 2004]. In addition, rate-and-state friction laws have been shown to describe the shear deformation and normal compaction of a wide variety of materials. Since the rate-and-state friction model appears to be experimentally robust and general, it seems probable that the law can be expanded to model deformation occurring under boundary conditions other than those imposed during laboratory friction experiments.

[3] Specifically, several different formulations of the rate-and-state equations exist for describing the fault-normal compaction typically observed during the so-called slide-hold-slide friction tests. A slide-hold-slide test is conducted by shearing a gouge layer or surface at a constant velocity (the slide phase), suddenly reducing the shearing velocity to zero (the hold phase) for an arbitrary period of time, and then suddenly resuming shearing at a constant velocity (the second slide phase). The fault-normal compaction observed under shear in unconsolidated gouge materials during holds in slide-hold-slide friction experiments is qualitatively similar to the volumetric creep compaction that occurs in unconsolidated sands and shales under hydrostatic compression [*Chang and Zoback*, 2003; *Hagin and Zoback*, 2004]. Both are characterized by compaction strain and strain rates that decay with time. For compaction of quartz sand in friction experiments [e.g., *Richardson and Marone*, 1999], strain rate decays according to a power law function of porosity during a hold. In volumetric creep tests on unconsolidated sands from the upper terminal zone of the Wilmington field (and others from the Gulf of Mexico), strain rate decays according to a power law of time, under conditions of hydrostatic stress [*Ostermeier*, 1995; *Chang et al.*, 1997; *Hagin and Zoback*, 2004].

[4] In this paper, we explore the possibility that rate-and-state friction laws can be used to describe the volumetric creep compaction of unconsolidated sands by expanding the standard rate-and-state formulation to include hydrostatic stress boundary conditions. First, we begin by finding appropriate stress and strain invariants to convert the rate-and-state equations from simple shear to hydrostatic stress boundary conditions. Second, existing volumetric creep data (from *Hagin and Zoback* [2004]) are replotted to show volumetric strain rate as a function of volumetric strain. Finally, the state-porosity relationship by *Segall and Rice* [1995] is used to test whether volumetric creep of unconsolidated sand can be described using rate-and-state friction laws.

2. Expanding Rate-and-State Friction Laws to Include Hydrostatic Stress Boundary Conditions

[5] We begin this section with a brief review of the rate-and-state friction formulation compiled by *Sleep* [1997,

[1]Stanford Stress and Crustal Mechanics Laboratory, Stanford University, Stanford, California, USA.

0148-0227/07/2006JB004286$09.00

1999, 2002]. After presenting the full formulation, the equations describing fault-normal compaction during an idealized hold (i.e., uniaxial compaction), we expand rate-and-state laws to include compaction under hydrostatic pressure. As the original formulation of rate-and-state friction is two dimensional, the expansion of the theory to include hydrostatic boundary conditions can be thought of as a partial description in three dimensions. A full three-dimensional derivation of the original rate-and-state friction theory is not required here.

2.1. Rate-and-State Friction

[6] While we made no measurements of frictional sliding in the laboratory studies reported here, we find it relevant to summarize the rate-and-state theory for frictional sliding to put our work on isotropic compaction in this context. The rate-and-state friction formalism was initially obtained from laboratory shearing experiments in which normal traction was held constant and friction was measured as a function of slip rate. In terms of macroscopic (observable in the laboratory) variables, the shear traction on a sliding surface depends on both the instantaneous rate of slip and a state variable that represents previous slip history [*Dieterich*, 1979; *Ruina*, 1983]. In our notation, the shear traction is

$$\tau = P[\mu_o + a\ln(V/V_o) + b\ln(\psi/\psi_{\mathrm{norm}})] \tag{1}$$

where μ_o is the steady state coefficient of friction, V is the sliding velocity, V_o is a reference velocity, and a and b are small dimensionless constants. The state variable ψ represents the real area of contact in the gouge layer, and the reference state ψ_{norm} is the steady state value of ψ when the fault is sliding at the reference velocity V_o. As shown below, ψ_{norm} represents the effect of changes in normal traction. Equation (1) can also be written in terms of strain and strain rate, which are more physically meaningful than gouge thickness and sliding velocity, even though they have not been directly measured in the laboratory. Following the work of *Sleep* [1997], this equivalent formulation can be written as

$$\tau = P\left[\mu_o + a\ln(\varepsilon\dot{Y}(x)/\varepsilon\dot{Y}_o) + b\ln(\psi(x)/\psi_{\mathrm{norm}})\right] \tag{2}$$

where strain rate $\varepsilon\dot{Y}(x)$ and state are functions of position within a gouge layer of finite thickness.

[7] Next, the evolution of the state variable must be explicitly defined in terms of slip distance and time in order for it to represent the effects of slip history on friction. While a variety of evolution equations exist, it is convenient to use the so-called "slowness" equation of *Dieterich* [1979] and *Linker and Dieterich* [1992], written in terms of macroscopic variables by *Sleep* [1997],

$$\frac{\partial\psi}{\partial t} = \frac{V_o P^N}{D_c P_o^N} - \frac{\psi V}{D_c} \tag{3}$$

where t is time, P_o is a reference normal traction, D_c is the critical displacement when the gouge layer is deforming uniformly (i.e., no strain localization), and N is related to the parameter $\alpha = bN$ of *Linker and Dieterich* [1992], which represents the effects of sudden changes in normal traction (see *Sleep et al.* [2000] for details). The critical displacement has been interpreted to represent the amount of slip required for the renewal of contacts between solid surfaces [*Marone and Kilgore*, 1993]. In terms of local variables, the state evolution equation can be written as

$$\frac{\partial\psi}{\partial t} = \frac{\varepsilon\dot{Y}_o(x)P^N}{\varepsilon_{\mathrm{int}}P_o^N} - \frac{\psi\varepsilon\dot{Y}(x)}{\varepsilon_{\mathrm{int}}} \tag{4}$$

where the critical strain $\varepsilon_{\mathrm{int}}$ is assumed to be an intrinsic material parameter and is defined such that $D_c = \varepsilon_{\mathrm{int}} \times W_{\mathrm{nom}}$, where W_{nom} is the thickness of the actively deforming part of the gouge layer.

2.2. Porosity and the State Variable

[8] At the most basic level, state is associated with dilatancy and compaction of a gouge layer [e.g., *Mair and Marone*, 1999; *Richardson and Marone*, 1999]. Results from many laboratory friction experiments suggest that the state variable can be related to the effective contact area of asperities in the active shear band [e.g., *Dieterich and Kilgore*, 1994] or to the energy available to dilate the gouge layer [*Beeler and Tullis*, 1997].

[9] Several authors have also argued that state represents porosity in the gouge layer [*Segall and Rice*, 1995; *Sleep*, 1997]. *Segall and Rice* [1995] expressed the state variable as a logarithmic function of porosity,

$$\phi - f = C_\varepsilon \ln(\psi) \tag{5}$$

where ϕ is a reference porosity at which $\psi = 1$, f is porosity, and C_ε is a dimensionless constant. *Sleep* [1997] arrived at a power law relationship between porosity and state by considering the evolution of porosity in the context of percolation theory [*Kirkpatrick*, 1973]. *Sleep* [1997] showed that his formulation is equivalent to that of *Segall and Rice* [1995] over a range of strain rates between 10^{-7} and 10^{-4} s^{-1}, which is the range of interest here, so the formulation of *Segall and Rice* [1995] is adopted because of its ease of use.

[10] Combining equations (4) and (5) results in an evolution equation for porosity, which includes the effects of sudden changes in normal traction and is independent of strain localization [*Sleep et al.*, 2000],

$$\frac{\partial f}{\partial t} = \frac{C_\varepsilon\varepsilon'(x)}{\varepsilon_m} - \frac{C_\varepsilon\varepsilon_o' P^N}{\psi(x)\varepsilon_{\mathrm{int}}P_o^N} \tag{6}$$

where the first term represents shear-enhanced dilatancy and the second represents time-dependent compaction. Now for the case of an "idealized" slide-hold-slide test in which shearing within the gouge is stopped for some amount of time and then restarted, it can be seen from equation (6) that, during the hold, the first term goes to zero (because the sliding rate goes to zero) and only the compaction term remains. Normal traction can be varied during the hold, but the P^N variables take this into account. Expanding the state variable in the time-dependent compaction term of equation (6) and eliminating the reference porosity (for the case of compaction without

prior shearing, the reference porosity ϕ is the initial porosity) gives,

$$\frac{\partial f}{\partial t} = \varepsilon \dot{Y}_c \frac{P_N}{P_o^N} \exp\left(\frac{-f}{C_\varepsilon}\right) \quad (7)$$

where C_ε and ε_{int} have been combined with the initial strain rate in the initial compaction rate variable f_c'. Refer to the works of *Sleep et al.* [2000] and *Sleep* [1997] for details.

[11] Equation (7) describes the time-dependent compaction of gouge under normal traction as a function of initial compaction rate, porosity, and pressure. Previous studies of volumetric compaction in unconsolidated sands under hydrostatic pressure [e.g., *Hagin and Zoback*, 2004] show that the compaction is functionally dependent on time, pressure, and porosity. In the next section, we modify equation (7) to include hydrostatic compression in order to test whether rate-and-state friction laws can be used to describe volumetric creep of unconsolidated sands.

2.3. Rate-and-State Representation of Hydrostatic Compression

[12] The mathematical details of the comparison between compaction under shear and normal stresses in laboratory friction tests and compaction under hydrostatic pressures in conventional triaxial tests are discussed in Appendix A. Note that the stress and strain invariants used in the comparison are only valid for isotropic materials. This is a valid assumption for the unconsolidated sand samples tested here, but not for a typical gouge layer that has experienced significant shear strain. However, prior to shearing, a typical quartz sand gouge is likely isotropic, so the equations presented in Appendix A should be thought of as valid for a gouge layer in which strain localization has not yet occurred (in other words, where the rate-and-state parameter "*a*" is greater than "*b*").

[13] Comparing the compaction that occurs under hydrostatic boundary conditions with that which occurs under the conditions of laboratory friction experiments results in the finding that they are approximately equal. This means that rate-and-state friction theory can be used to describe hydrostatic creep compaction and, furthermore, that the parameter values recovered in fitting data from hydrostatic creep tests to rate-and-state theory are directly comparable to values recovered from data from traditional slide-hold-slide friction tests. For a description of the slide-hold-slide test, see for example the work of *Dieterich* [1972]. In the next section, results from a series of hydrostatic creep experiments designed for compatibility with rate-and-state theory are discussed.

3. Laboratory Studies and Model Verification

[14] To verify that modified rate-and-state friction laws are an appropriate choice for modeling the volumetric compaction of unconsolidated sands, hydrostatic creep tests were conducted at a variety of pressures and pressurization rates. Volumetric creep strain is simply an inelastic deformation that occurs under constant pressure conditions. Tests were conducted on samples of unconsolidated reservoir sand from the Wilmington field in California and synthetic samples prepared in the laboratory using mixtures of disaggregated Ottawa sand and wetted montmorillonite clay. All samples were cleaned with solvents and dried in a vacuum oven prior to testing and were trimmed to 1-inch diameter, 2-inch long right cylinders. Plugs of the unconsolidated Wilmington sand were obtained from 4-inch diameter core, collected in the upper terminal zone of the Wilmington field at a depth of approximately 1 kilometer. The samples were outfitted with two linear potentiometers (each with a stroke of 12.5 mm) to measure axial displacement, an LVDT-based chain gauge to measure radial displacement, and the top and bottom of the sample were plumbed with hydraulic lines to enable drainage of the pore space to ambient atmospheric pressure. All of the experiments were hydrostatic compression tests on dry samples without pore fluids or elevated pore pressure, under room temperature and humidity conditions. All tests were conducted using an NER Autolab 2000 conventional triaxial press, with command signal feedback configured such that the hydrostatic pressure (supplied by a mineral oil bath) was controlled by the volumetric strain.

[15] Creep strain tests were selected such that the rate-and-state parameters C_ε and N could be solved [refer back to equation (7)]. As any volumetric creep test will supply the data needed to find C_ε (strain rate as a function of strain), it is only necessary to measure volumetric creep strain as a function of hydrostatic pressure in order to find the parameter N of *Linker and Dieterich* [1992]. In addition, experimental evidence shows that the initial conditions in a gouge affect the values of the rate-and-state variables. *Sleep et al.* [2000] suggested that the normal compaction of a gouge during a hold depends on the history prior to the hold. We attempted to take this into account by varying the stress rate (pressurization rate) prior to the start of the creep test. For this study, creep tests were conducted at pressures ranging from 5 to 30 MPa and at stress rates between 10^{-7} and 10^{-2} MPa s^{-1}. An example of a typical stress-strain history used for these experiments is shown and explained in Figure 1.

3.1. Modeling Strain-Rate Decay in Unconsolidated Sands

[16] Replotting the creep data in Figure 1 in terms of volumetric strain rate and porosity instead of volumetric strain and time makes it possible to test whether or not rate-and-state friction theory succeeds in describing the data. While the majority of samples tested were unconsolidated sand from the Wilmington field, several tests were conducted on disaggregated Ottawa sand to facilitate comparison of data from tests on quartz sand samples typically used in rate-and-state tests. Ottawa sand is mineralogically more similar to quartz sand than the relatively clay-rich Wilmington sand, and it is desirable to isolate any effects of mineralogy on the compaction data.

[17] As a reminder, the logarithmic relation of *Segall and Rice* [1995] between porosity and state [equation (7)] is used here. In a typical slide-hold test, the gouge layer is in motion before the hold. In order to best simulate this condition, the samples in our hydrostatic tests were compacted at some slow loading rate prior to holding the pressure constant in the creep tests, and the data from these tests are presented here. As mentioned previously, the effect of prior history (loading rate or pressurization

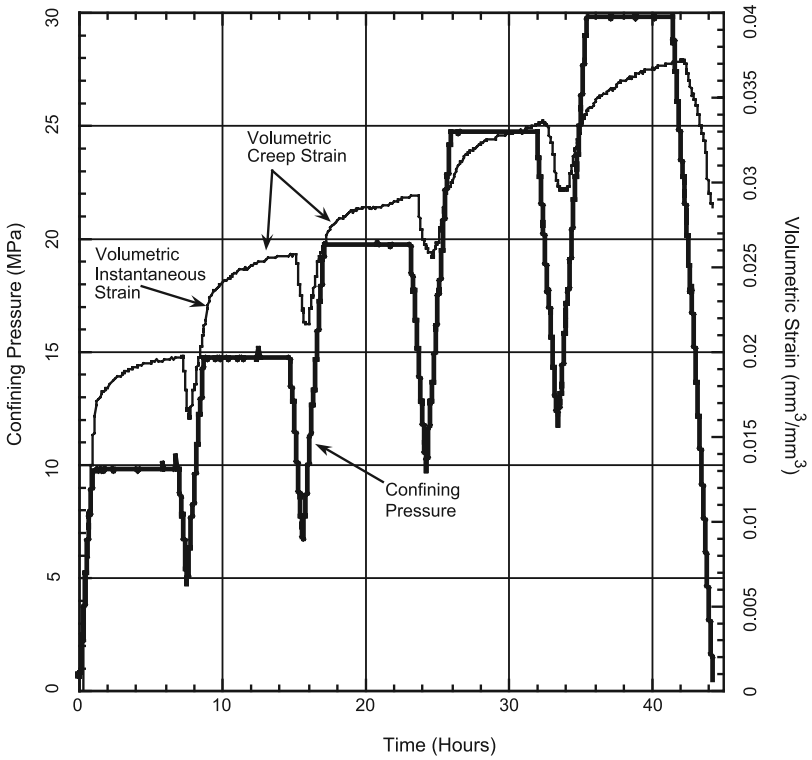

Figure 1. Plot of pressure and volumetric strain versus time from a series of creep compaction tests conducted under hydrostatic stress conditions on room-dry unconsolidated Wilmington sand. The sample was pressurized at a rate of 5 MPa/hour and then allowed to creep under constant pressure for 6 hours before being partially unloaded and then loaded to the next pressure step. The samples were partially unloaded in an attempt to prevent the creep signal for a particular pressure step from interfering with the creep strain observed during future steps. For this study, creep tests were conducted at various pressures, pressure steps, and loading rates.

rate) on a sample during a hold is relatively unknown, so creep tests were conducted at a variety of initial loading rates. Loading rate appears to have a significant impact of the value of C_ε, but the results are inconclusive. A summary of C_ε as a function of loading rate is presented in Appendix B.

[18] From equation (7), rate-and-state theory predicts that volumetric strain rate should decay as an exponential function of porosity. Figure 2 shows creep strain data from a Wilmington sand sample compressed at a stress rate of $\sim 10^{-4}$ MPa s^{-1} to 30 MPa, replotted as volumetric strain rate versus porosity ($\sim$volume strain). Plotting the data in log linear space reveals that the predicted exponential decay is observed. By fitting the data using equation (7), the value of C_ε can be determined, and in this case, it is approximately 18×10^{-4}.

[19] Tests on samples of disaggregated Ottawa sand show similar behavior, as seen in Figures 3 and 4. The values of C_ε recovered for pure Ottawa sand and a mixture of sand and montmorillonite clay are approximately equal to the value recovered for Wilmington sand. This suggests that C_ε is relatively independent of mineralogy and grain characteristics such as size and angularity. In addition, C_ε appears to be independent of confining pressure. Performing a series of creep tests on a single sample of Wilmington sand under monotonically increasing pressure steps of 5 MPa between 10 and 30 MPa results in a mean C_ε value of 20×10^{-4} and a standard deviation of 3×10^{-4}. The values of C_ε recovered from all of these tests are summarized in Table 1, and the data are shown in Figure 5.

3.2. Modeling the Effect of Sudden Pressure Changes on Unconsolidated Sands

[20] Examining equations (6) and (7) once more, notice that two material parameters need to be found experimentally, C_ε and N. The creep tests in the previous section provided the values for C_ε but not N because the tests were all conducted at constant pressure and sudden changes in pressure are required. On the other hand, results from the previous section showed that C_ε is a nearly constant function of pressure, which provides a means for determining N. By assuming that C_ε is constant and suddenly changing the pressure during a creep test, N can be determined.

[21] The results presented here were obtained from experiments identical to those depicted in Figure 1, except that the hydrostatic pressure was increased suddenly (at 2 MPa s^{-1}) after 6 hours of creep strain. The initial pressure for each test was 10 MPa, loaded at 2 MPa s^{-1}, and pressures were increased to 15, 20, 25, and 30 MPa. Equation (6) predicts that the initial volumetric strain rate following a step

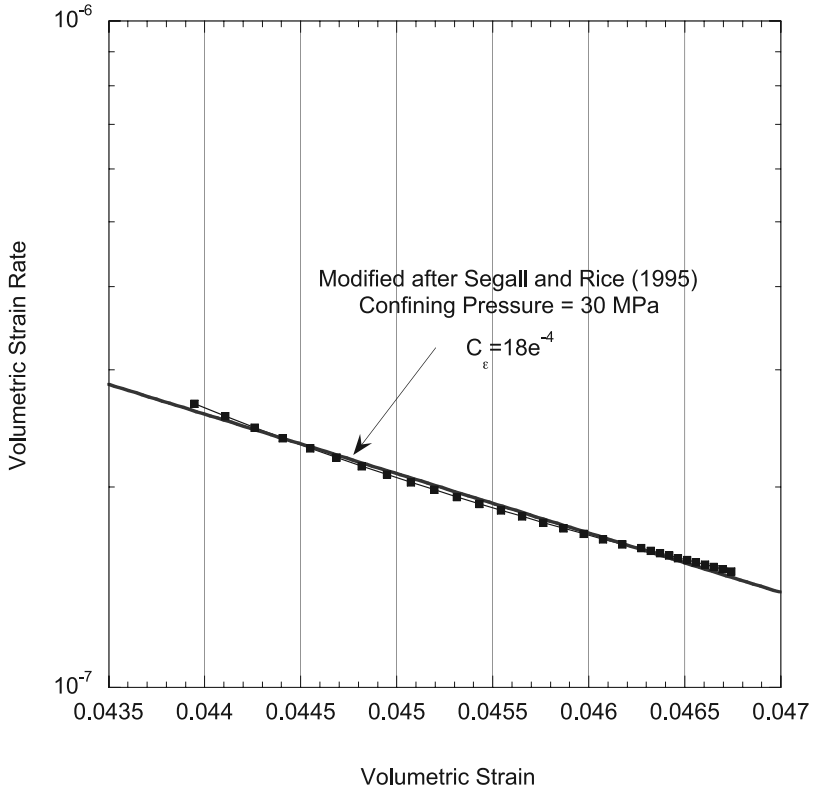

Figure 2. Plotting volumetric creep data as volumetric strain rate versus strain allows the rate-and-state parameter C_ε to be determined. Here creep strain data from an unconsolidated Wilmington sand sample is shown.

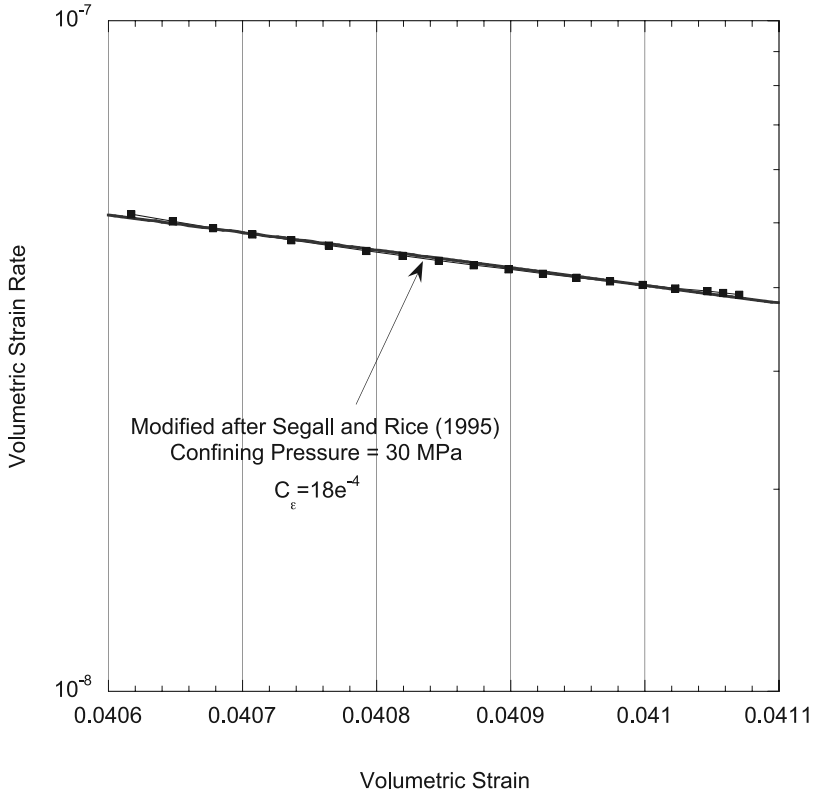

Figure 3. Volumetric creep data for an Ottawa sand sample. The value of C_ε is approximately equal to the value measured for Wilmington sand despite differences in mineralogy.

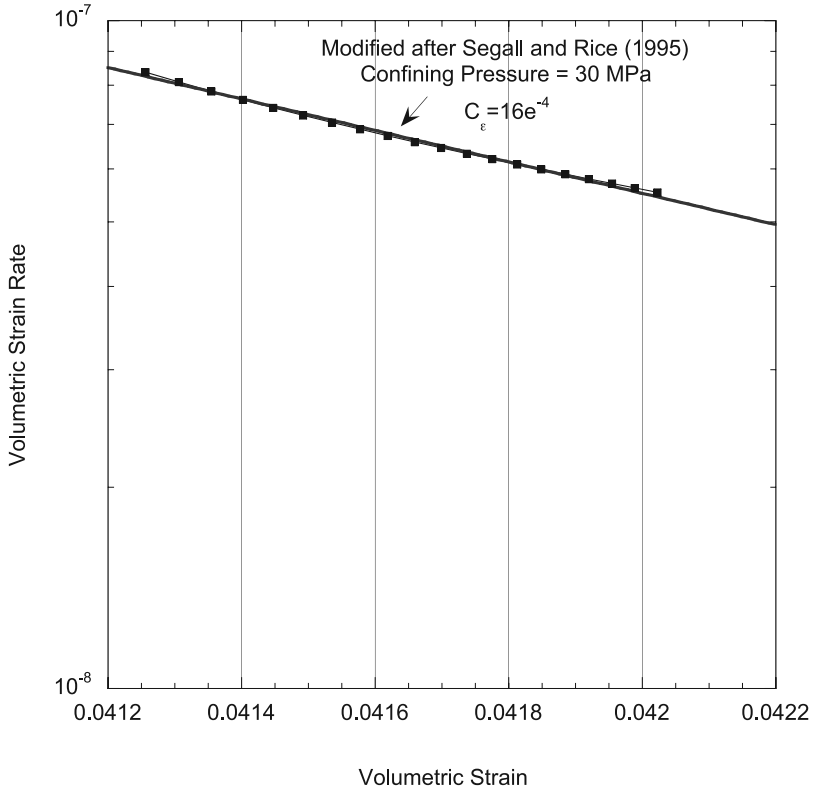

Figure 4. Volumetric creep data for an Ottawa sand sample with 10% montmorillonite clay. Value of C_ε measured here is approximately equal to the value obtained for a pure Ottawa sample.

increase in pressure should be a power law function of the normalized change in pressure. N is determined by fitting a power law to the initial volumetric strain rate plotted against the ratio of the new pressure to the original pressure, as shown in Figure 6.

[22] Figure 6 shows that the initial volumetric strain rate data do indeed follow a power law function of the pressure ratio. Fitting the data to find the power of N yields the following equation,

$$\varepsilon \dot{Y}_o = 3.52e^{-7} \times \left(\frac{P}{P_o}\right)^9 \tag{8}$$

where N is equal to 9 ± 2, and εY_o is the initial volumetric strain rate.

4. Discussion

[23] *Sleep et al.* [2000] obtained a C_ε value of $28-56 \times 10^{-4}$ for quartz sand gouge in a slide-hold test under direct shear boundary conditions, which compares well with the values recovered from unconsolidated sand samples under hydrostatic compression in this study. This finding means that conducting hydrostatic compression tests, which are relatively simple compared with laboratory friction tests, can reliably identify C_ε values.

[24] We suspect that the real contact areas in our hydrostatic creep tests also increased more rapidly than one would infer from sliding experiments, implying that our measured value of N should be lower than values obtained from friction experiments. Real contact areas at asperities increase more rapidly during holds in friction tests than one would infer by measuring friction after sliding resumes or after changes in sliding velocity [*Dieterich and Kilgore*, 1994; *Goldsby et al.*, 2004]. The first increment of shear strain before friction peaks at the restart of sliding after the holds destroys some of the real area of contact, weakening the gouge without changing porosity.

[25] Mathematically, we are approximating exponential creep [*Nakatani and Scholz*, 2004] at asperity contacts with a power law creep in equation (7). For this to work we need the strain rate for both flow laws to be the same at the real stress σ for the expansion

$$f' = f_1' \exp(\sigma/\sigma_0) = f_1' \left[\frac{\sigma}{\sigma_1}\right]^N \tag{9}$$

where f_1' is a constant with the dimensions of strain rate, σ_0 is a material constant with dimensions of stress, and the

Table 1. Compilation of Compaction Coefficients

Sample Type	P_c (MPa)	Initial Volume Strain	C_ε
Wilmington	30	0.8×10^{-3}	18×10^{-4}
"	25	1.1×10^{-3}	15×10^{-4}
"	20	2.2×10^{-3}	12×10^{-4}
"	15	4.0×10^{-3}	18×10^{-4}
"	10	8.2×10^{-3}	21×10^{-4}
Ottawa	30	5×10^{-8}	18×10^{-4}
Ottawa/10% clay	30	8.6×10^{-8}	16×10^{-4}

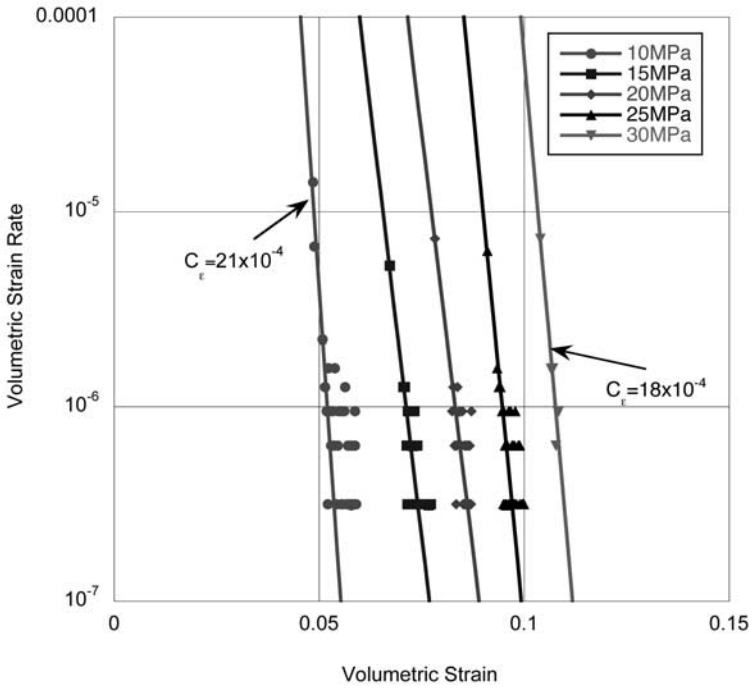

Figure 5. Volumetric creep data for a sample of Wilmington sand as a function of confining pressure. C_ε appears to be independent of pressure over a range of confining pressures from 10 to 30 MPa.

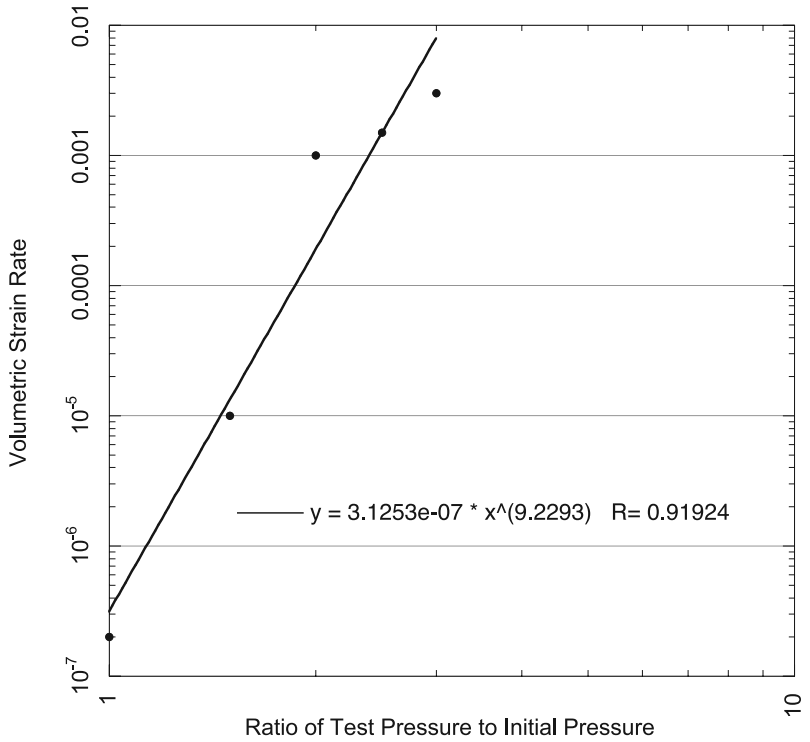

Figure 6. The parameter "N", proportional to the parameter α introduced by *Linker and Dieterich* [1992], can be determined by measuring strain rate in response to sudden changes in pressure. Volumetric strain rate should follow a power law function of the ratio of test pressure to initial pressure, where the power is N. For Wilmington sand, N is approximately 10 (N = 9.2293 in the figure).

equality determines the stress σ_1. The (logarithmic) derivatives to strain rate must also be equal,

$$\frac{\partial[\ln f']}{\partial\sigma} = \frac{1}{\sigma_0} = \frac{N}{\sigma} \tag{10}$$

This gives the power law exponent in terms of the real stress and a material property

$$N = \sigma/\sigma_0 \tag{11}$$

[26] Our experimental data suggest that N is approximately 10 for Wilmington sand. This result represents a reasonable agreement with the value of N found by *Sleep et al.* [2000], who obtained a value of 20 ± 10. We note that the appropriate range for values of N is difficult to judge because there are so few values of N reported in the literature. This result implies that parameters for the rate-and-state compaction equation (6) for different materials can be found just by conducting hydrostatic compression tests. Interestingly, the value of N recovered here also fits within the range of values obtained by *Linker and Dieterich* [1992] during slide-hold-slide tests on granite blocks ($10 \leq N \leq 40$).

[27] We can qualitatively explain why our value of $N \sim 10$ is at the low end of the data compiled from slide-hold-slide experiments. *Goldsby et al.* [2004] conducted single-contact indentation creep experiments on quartz, obtaining data on the area of contact as a function of time (see their Figure 7) that follows an equation of the form

$$\frac{\partial(A/A_0)}{\partial[\ln(t)]} = \chi \tag{12}$$

where A/A_0 is the area of contact normalized to its value at some time and χ is the slope of their graph. Their value of ψ (state) at the end of their indentation creep "holds" is 1.7 times that inferred from slide-hold-slide experiments on quartz rocks. Applying this information to our experiments, the real stress σ (which scales inversely to real contact area) should be a factor of 1/1.7 of that in sliding experiments. That is, we predict from our results and equation (11) that N in sliding experiments is $\sim$17. This is in better agreement with our compiled friction data than our value of 10.

[28] *Goldsby et al.* [2004] obtained and compiled real contact stresses for quartz from 7 to 14 GPa. Our Wilmington samples contain clay, which should have a lower real contact stress than pure quartz. In addition, the material property σ_0 should not vary greatly between silicates at seismogenic conditions. It is $\approx RT/M$ where R is the gas constant, T is absolute temperature, and M is the effective molecular volume of the rate-limiting step of creep. Using the molecular volume of quartz, 2×10^{-5} m^3 mol^{-1}, yields 110 MPa for our room temperature experiment. This gives from equation (11) a real stress of 1.1 MPa. This is too low for intact quartz. It may be appropriate if a weak material like clay or hydrated silica creeps at real contacts [*Frye and Marone*, 2002; *Di Toro et al.*, 2004], rather than if dry quartz creeps.

[29] Note that *Ruina* [1983] proposed an alternative evolution law where no compaction or change of the state variable occurs during a hold. This law applies during some experimental situations like simulated gouge under low humidity [*Frye and Marone*, 2002]. Its null prediction is not applicable to time-dependent hydrostatic compaction of sand.

[30] We have shown that it is possible to describe creep compaction under hydrostatic compression using slightly modified rate-and-state friction theory. Comparing the original rate-and-state equations with equations modified to use stress and strain invariants appropriate for hydrostatic compression results in the finding that the two equations predict the same compaction, or that compaction is almost invariant of boundary conditions. More significantly, in fitting creep strain data under constant hydrostatic stress boundary conditions, values for the rate parameter C_ε and the parameter N of *Linker and Dieterich* [1992] recovered here reasonably match those found by *Sleep et al.* [2000] when fitting the normal compaction of quartz sand gouge under double-direct shear boundary conditions. The fact that rate-and-state friction theory succeeds in describing data collected under boundary conditions very different from those used in its original formulation shows that it is robust and general. Furthermore, the observation that the values of C_ε and N are similar for different materials under different boundary conditions suggests that rate-and-state friction theory is revealing something about the intrinsic physical properties of the materials, although these properties may not be determined directly using traditional experimental methods.

[31] Another important result from this study is that some rate-and-state parameters, at least C_ε and N, can now be determined easily for a wide variety of materials. The finding that hydrostatic data can be used to recover values for rate-and-state parameters significantly increases the amount of data available in the literature for cataloging these parameters for a variety of materials.

[32] Our finding that C_ε is nearly constant as a function of pressure is consistent with classical friction theory. This implies that the normal stress acting on the active contacts in a gouge layer is approximately independent of the normal stress applied externally and that the contact-stress-driven yielding of the gouge is also independent of normal stress. This is the expected result from friction theory (e.g., *Bowden and Tabor*, 1954).

[33] There has been some discussion in the literature about the nature of the normal compaction that occurs during hold tests [e.g., *Nakatani*, 1998]. *Marone et al.* [1990] argued that all changes in porosity are due to shear. *Beeler and Tullis* [1997] provided evidence for time-dependent compaction. Our results lend support to the idea that compaction during holds is truly time dependent. We observe time-dependent compaction under hydrostatic stress conditions that can be modeled using rate-and-state friction theory.

[34] During an idealized hold, the shear strain rate in the gouge and the first term of equation (6) would go to zero instantaneously. This leaves an equation that describes the time-dependent compaction of the gouge as a function of normal stress, reference shear strain rate, the distribution of state across the layer, and a compaction/dilation

constant $C_\varepsilon \varepsilon_{\text{int}}$. The shear strain rate prior to the hold does not factor into the compaction occurring during the hold. Likewise, the shear stress acting on the gouge layer during the hold does not affect the compaction. In other words, equation (6) accurately describes the compaction of the gouge layer even when the shear stress and shear strain rate are zero, that is, the compaction starts at rest under purely normal stress boundary conditions. For a real hold during a slide-hold-slide friction test, shear stresses will be acting on the gouge layer and the shear strain rate will be nonzero, resulting in the first term of equation (6) being positive. Equation (7) then becomes an approximation that is valid when the shear strain rate decays rapidly as a function of strain.

[35] An interesting application for the hydrostatic compression version of the rate-and-state friction equations developed here would be to try to describe the compaction and deformation of reservoirs and aquifers. The hydrostatic form of the rate-and-state equations can be used to relate changes in pressure to volumetric strain rate and porosity, so theoretically, it should be possible to use it for reservoir geomechanics. In addition, the traditional form of the rate-and-state equations could be used to simultaneously predict the slip and compaction of any reservoir-bounding faults. This opens up the possibility of a unified and systematic approach to both friction and compaction in reservoirs.

5. Conclusions

[36] Rate-and-state friction laws have been shown to describe the fault-normal compaction that occurs during holds in slide-hold-slide friction tests on unconsolidated gouge materials. This compaction is qualitatively similar to that observed during volumetric creep tests on unconsolidated sands and shales under hydrostatic loading conditions. In an attempt to model the volumetric creep data, the rate-and-state friction equation is modified to include compaction under hydrostatic stress boundary conditions. Results show that the hydrostatic stress form of the rate-and-state law successfully describes volumetric creep of unconsolidated sand. This is significant because hydrostatic compaction is time dependent, which suggests that the fault-normal compaction occurring during holds in slide-hold-slide tests is also time dependent, rather than slip dependent. Also, we recover values of the rate-and-state parameter C_ε that are independent of pressure, in agreement with classical friction theory.

Appendix A: Representing Hydrostatic Compression Using Rate-and-State Theory

[37] The first goal is to rewrite the compaction terms of the rate-and-state equations in terms of stress and strain invariants. The second goal is to compare the amount of compaction predicted by the rate-and-state friction equations with the measured compaction of unconsolidated sands in a hydrostatic creep test. The strain rate described by the rate-and-state equation is engineering shear strain rate, which needs to be written in terms of invariants to allow the comparison.

[38] The isotropic stress and strain rate tensors are defined as

$$\begin{aligned} P &= -\sigma_{ii}, \\ \Delta &= \varepsilon \acute{Y}_{ii}, \end{aligned} \tag{A1}$$

the deviatoric stress and strain rate tensors are

$$\begin{aligned} T_{ij} &= \sigma_{ij} + P, \\ e\acute{Y}_{ij} &= \varepsilon \acute{Y}_{ij} - \tfrac{1}{3}\Delta, \end{aligned} \tag{A2}$$

and the engineering convention for stress is assumed (tension is positive).

[39] Next, the deviatoric strain rate tensor is manipulated such that it reduces to engineering shear strain rate under simple shear boundary conditions. For simple shear, the engineering strain rate is twice the deviatoric strain rate,

$$e\acute{Y}_{ij} = \varepsilon \acute{Y}_{ij} = e\acute{Y}_{xz} = \frac{1}{2} E_{\acute{Y}} \tag{A3}$$

and the deviatoric strain rate tensor can be written as follows,

$$|e\acute{Y}| = \sqrt{2 e\acute{Y}_{ij} e\acute{Y}_{ij}} = \sqrt{2\left[2\left(\frac{1}{2}E^{\acute{Y}}\right)^2\right]} = E^{\acute{Y}} \tag{A4}$$

Having found an appropriate way to write the engineering shear strain rate in terms of invariants, the rate-and-state fault-normal compaction term can now be compared with the time-dependent volumetric compaction due to hydrostatic compression. Starting with the isotropic strain rate tensor,

$$\begin{aligned} &\Delta = \varepsilon \acute{Y}_{ii} = \varepsilon \acute{Y}_{zz} \text{ (Normal Compaction), and} \\ &\Delta = D = \frac{-\partial f}{\partial t} \text{ (Pure Compaction),} \end{aligned} \tag{A5}$$

where $\Delta = D$ represents the case of pure compaction without shear (i.e., during an idealized hold) in which all of the compaction closes porosity. Next, the engineering shear strain rate can be calculated from equation (A3),

$$\begin{aligned} e\acute{Y}_{ij} &= \begin{vmatrix} \frac{1}{3}D & 0 & 0 \\ 0 & \frac{1}{3}D & 0 \\ 0 & 0 & \frac{2}{3}D \end{vmatrix}, \\ \left|e\acute{Y}^2\right| &= 2\left(\tfrac{2}{3}D\right)^2 + 4\left(\tfrac{1}{3}D\right)^2, \\ E^{\acute{Y}} &= \left|e\acute{Y}\right| = \frac{\sqrt{3}2D}{3}, \end{aligned} \tag{A6}$$

where the deviatoric strain rate tensor (the D terms) is chosen such that Poisson's ratio is preserved ($\upsilon = 0.5$).

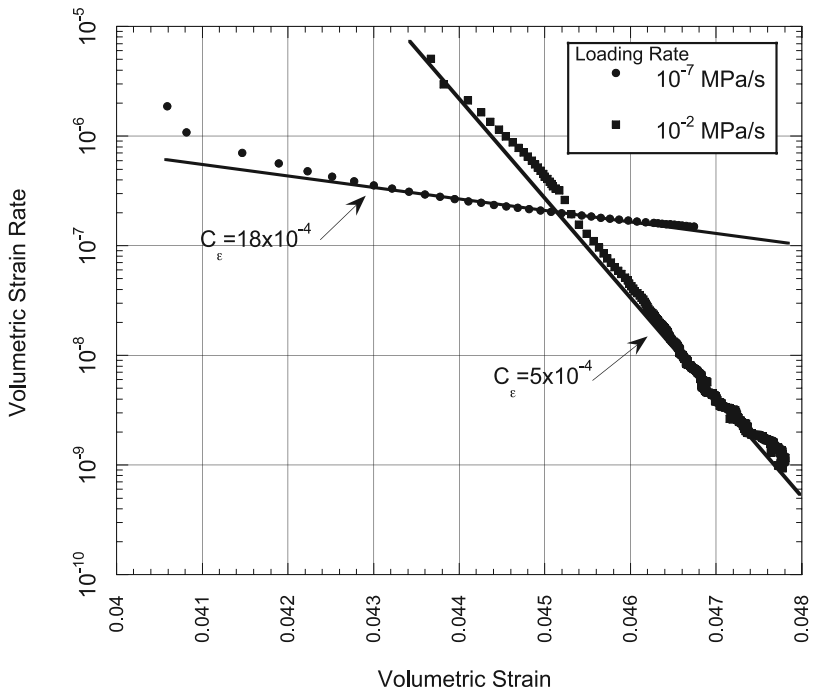

Figure B1. Effect of initial loading rate on the value of the rate-and-state parameter C_ε. C_ε decreases as initial loading rate increases. For the range of loading rates used here, C_ε can be seen to decrease by nearly an order of magnitude.

[40] The next step in comparing the rate-and-state compaction with hydrostatic creep compaction is to write the evolution equation for porosity in terms of the engineering shear strain D (porosity change predicted from rate-and-state theory) and D_{com}, the measured porosity change. Starting with equation (6), the porosity evolution equation (substituting in for the D terms) is

$$-D = \frac{-C_\varepsilon E^{\dot{Y}}}{\varepsilon_{\text{int}}} + D_{\text{com}}, \tag{A7}$$

and the engineering shear strain can be represented in terms of D, from equation (A6), to give

$$-D = \frac{-C_\varepsilon}{\varepsilon_{\text{int}}} \frac{2\sqrt{3}D_{\text{com}}}{3} + D_{\text{com}}. \tag{A8}$$

Rewriting equation (A8) slightly allows for a direct comparison between D and D_{com},

$$D = D_{\text{com}}\left(1 - \frac{2\sqrt{3}C_\varepsilon}{3\varepsilon_{\text{int}}}\right), \tag{A9}$$

and because the bracketed term is approximately equal to 1 (*Sleep et al.* [2000] found that the ratio $C_\varepsilon/\varepsilon_{\text{int}}$ is between 0.028 and 0.056),

$$D \cong D_{\text{com}} \tag{A10}$$

which implies that the compaction predicted to occur during a hold test is approximately the same as the pure compaction measured during a hydrostatic compression creep strain test.

Appendix B: Loading Rate Effects on the Rate-and-State Friction Parameter C_ε

[41] The effect of initial loading rate on the rate-and-state friction parameter C_ε was explored by running a series of tests during which only the initial loading rate was varied. Initial loading rates varied by several orders of magnitude, approximately from 10^{-7} to 10^{-2} MPa s^{-1}. Representative data at the extreme ends of this range for Wilmington sand are shown in Figure B1. The data taken at an initial loading rate of 10^{-7} MPa s^{-1} are the same data as shown in Figure 1 and produce a C_ε value of 18×10^{-4}. On the other hand, the data taken at an initial loading rate of 10^{-2} MPa s^{-1} produce a C_ε value of 5×10^{-4}, a difference of approximately a factor of four. Disaggregated Ottawa sand produces similar results, with C_ε values of 18×10^{-4} and 3×10^{-4} at loading rates of 10^{-7} and 10^{-2} MPa s^{-1}, respectively.

[42] This difference in C_ε as a function of initial loading rate is not easily explained. At first, it was suspected that grain crushing at higher loading rates was responsible for the lower C_ε values. However, microstructural analyses of deformed samples revealed that there was no discernable difference in grain size distribution either between samples tested at different loading rates or between tested and untested samples. One possible explanation for the observed variation of C_ε is that individual grains are locking together rather than sliding past one another at higher initial loading rates; this might cause a so-called ''arch support'' effect

which would protect the interior of the sample from changes in stress and result in a rapid decay of strain rate.

[43] A typical slide-hold-slide test involves starting the hold after deforming a sample under shear at some finite rate. To best simulate this with the hydrostatic compaction tests performed in this study, we chose the data from tests run at slow initial loading rates, because of the greater likelihood that the entire sample would be deforming at the start of the hold, thereby reducing any effect of "arch support". However, even if the higher loading rate data had been used, the C_ε values obtained would still have been within the range of values reported in the literature. *Segall and Rice* [1995] reported a value on the order of 2×10^{-4}, although they did not take into account the effect of strain localization, which would introduce an error such that their measured value would be smaller than the actual value. In any case, understanding how C_ε varies as a function of initial conditions remains an important and outstanding issue.

[44] **Acknowledgments.** This research was supported by the Southern California Earthquake Center (SCEC). SCEC is funded by NSF Cooperative Agreement EAR-0106924 and USGS Cooperative Agreement 02HQAG0008. The SCEC contribution number for this paper is 946. Nick Beeler and Steve Karner provided comments that greatly improved an early version of this manuscript. Comments from Chris Marone helped to improve both the clarity of the ideas presented here and the science behind them.

References

Beeler, N. M. (2004), Review of the physical basis of laboratory-derived relations for brittle failure and their implications for earthquake occurrence and earthquake nucleation, *Pure Appl. Geophys.*, *161*(9–10), 1853–1876.

Beeler, N. M., and T. E. Tullis (1997), The roles of time and displacement in the velocity-dependent volumetric strain of fault zones, *J. Geophys. Res.*, *102*, 22,925–22,609.

Bowden, F. P., and D. Tabor (1954), *Friction and Lubrication of Solids*, Oxford Univ. Press, New York.

Chang, C., and M. D. Zoback (2003), Creep compaction in Gulf of Mexico shales, *SRB Ann. Meeting Proc.*, *76*, Paper C-3.

Chang, C., D. Moos, and M. D. Zoback (1997), Anelasticity and dispersion in dry unconsolidated sands, *Int. J. Rock Mech. Min. Sci.*, *34*(3/4), 402.

Dieterich, J. H. (1972), Time-dependent friction in rocks, *J. Geophys. Res.*, *77*, 3690–3697.

Dieterich, J. H. (1978), Time-dependent friction and the mechanics of stick-slip, *Pure Appl. Geophys.*, *116*, 790–806.

Dieterich, J. H. (1979), Modeling of rock friction: 1. Experimental results and constitutive equations, *J. Geophys. Res.*, *84*(B5), 2161–2168.

Dieterich, J. H., and B. D. Kilgore (1994), Direct observation of frictional contacts: New insights for state-dependent properties, *Pure Appl. Geophys.*, *143*, 387–423.

Di Toro, G., D. L. Goldsby, and T. E. Tullis (2004), Friction falls toward zero in quartz rock as slip velocity approaches seismic rates, *Nature*, *427*(6973), 436–439.

Frye, K. M., and C. Marone (2002), The effect of humidity on granular friction at room temperature, *J. Geophys. Res.*, *107*(B7), 2309, doi:10.1029/2001JB000654.

Goldsby, D. L., A. Rar, G. M. Pharr, and T. E. Tullis (2004), Nanoindentation creep of quartz, with implications for rate- and state-variable friction laws relevant to earthquakes mechanics, *J. Mater. Res.*, *19*(1), 357–365.

Hagin, P., and M. D. Zoback (2004), Viscous deformation of unconsolidated reservoir sands: Part 1. Time-dependent deformation, frequency dispersion, and attenuation, *Geophysics*, *69*, 731–741.

Kirkpatrick, S. (1973), Percolation and conduction, *Rev. Mod. Phys.*, *45*, 574–588.

Linker, M. F., and J. H. Dieterich (1992), Effects of variable normal stress on rock friction: Observations and constitutive equations, *J. Geophys. Res.*, *97*, 4923–4940.

Mair, K., and C. Marone (1999), Friction of simulated fault gouge for a wide range of velocities and normal stress, *J. Geophys. Res.*, *104*, 28,899–28,914.

Marone, C., and B. Kilgore (1993), Scaling of the critical slip distance for seismic faulting with shear strain in fault zones, *Nature*, *362*, 618–621.

Marone, C., C. B. Raleigh, and C. H. Scholz (1990), Frictional behavior and constitutive modeling of simulated fault gouge, *J. Geophys. Res.*, *95*, 7007–7025.

Nakatani, M. (1998), A new mechanism of slip-weakening and strength recovery of friction associated with mechanical consolidation of gouge, *J. Geophys. Res.*, *103*, 27,239–27,256.

Nakatani, M. (2001), Conceptual and physical clarification of rate and state friction: Frictional sliding as a thermally activated rheology, *J. Geophys. Res.*, *106*(B7), 13,347–13,380.

Nakatani, M., and C. Scholz (2004), Frictional healing of quartz gouge under hydrothermal conditions: 2. Quantitative interpretation with a physical model, *J. Geophys. Res.*, *109*(B7), B07202, doi:10.1029/2003JB002938.

Ostermeier, R. M. (1995), Deepwater Gulf of Mexico turbidites—Compaction effects on porosity and permeability, *SPE Form. Eval.*, 79–85.

Rice, J. R., N. Lapusta, and K. Ranjith (2001), Rate- and state-dependent friction and the stability of sliding between elastically deformable solids, *J. Mech. Phys. Solids*, *49*(9), 1865–1898.

Richardson, E., and C. Marone (1999), Effects of normal force variations on frictional healing, *J. Geophys. Res.*, *104*, 28,859–28,878.

Ruina, A. (1983), Slip instability and state variable friction laws, *J. Geophys. Res.*, *88*, 10,359–10,370.

Segall, P., and J. R. Rice (1995), Dilatancy, compaction, and slip-instability of a fluid-penetrated fault, *J. Geophys. Res.*, *100*(101), 22,155–22,171.

Sleep, N. H. (1997), Application of a unified rate and state friction, *J. Geophys. Res.*, *102*, 2875–2895.

Sleep, N. H. (1999), Rate- and state-dependent friction of intact rock and gouge, *J. Geophys. Res.*, *104*, 17,847–17,855.

Sleep, N. H. (2002), Self-organization of crustal faulting and tectonics, *Int. Geol. Rev.*, *44*, 83–96.

Sleep, N. H., E. Richardson, and C. Marone (2000), Physics of friction and strain rate localization in synthetic fault gouge, *J. Geophys. Res.*, *105*, 25,875–25,890.

Yale, D. P., G. W. Nabor, J. A. Russel, H. D. Pham, and M. Yous (1993), Application of variable formation compressibility for improved reservoirs analysis: SPE-26647, in SPE Annual Technical Conference Proceedings: Society for Petroleum Engineers.

P. Hagin, N. H. Sleep, and M. D. Zoback, Stanford Stress and Crustal Mechanics Laboratory, Stanford University, Stanford, CA, USA. (hagin@pangea.stanford.edu)